


Equations of magnetic field of transformer steel sheets

WITOLD MAZGAJ ¹✉, MICHAŁ SIERŻĘGA ²

¹*Department of Electrical Engineering, Cracow University of Technology
Warszawska 24 str., 31-155 Kraków, Poland*

e-mail: ✉ pemazgaj@cyfronet.pl, michal.sierzega@pk.edu.pl

(Received: 02.05.2024, revised: 16.11.2024)

Abstract: This study described a method for determining the magnetic field in transformer steel sheets for any magnetisation direction. In the proposed approach, limiting hysteresis loops for the rolling and transverse directions were used. These loops, which were determined separately in both directions, were modified depending on the direction of magnetisation. The assumed area of the magnetic field occurrence was divided into elementary segments, and the appropriate components of field strength and flux density were assigned to the edges and elementary segments of the grid dividing this area. The relationships between the flux density and field strength along both the rolling and transverse directions in the elementary segments were introduced into the equations of the magnetic field distribution, which were based on Maxwell's equations in the integral form. These equations facilitated the determination of changes in the magnetic field, considering the magnetic hysteresis. The correctness of these equations was validated through comparisons of the results of numerical calculations with the analogous results of measurements performed using a laboratory package of transformer sheets.

Key words: equation of magnetic field, Goss texture, hysteresis loop, magnetisation process, transformer steel sheet

1. Introduction

In many cases, the magnetic field is considered a one-dimensional field in significant parts of the transformer cores. However, this statement is not applicable to the corners and T-joint areas because the magnetic field lines change their direction and the magnetic field exhibits a nature to that of a two-dimensional field (Fig. 1). Certain studies have indicated that changes in the magnetic field in these areas can be regarded as elliptical rotational magnetisation. This is primarily owing to the phenomenon of magnetic hysteresis occurring in electrical steel sheets, and both the field



© 2024. The Author(s). This is an open-access article distributed under the terms of the Creative Commons Attribution-NonCommercial-NoDerivatives License (CC BY-NC-ND 4.0, <https://creativecommons.org/licenses/by-nc-nd/4.0/>), which permits use, distribution, and reproduction in any medium, provided that the Article is properly cited, the use is non-commercial, and no modifications or adaptations are made.

strength and flux density vectors are not collinear. In such cases, the power loss should be estimated using the following general formula in a rectangular coordinate system [1]:

$$P = \frac{1}{T} \int_0^T \left(H_x \frac{dB_x}{dt} + H_y \frac{dB_y}{dt} \right) dt, \quad (1)$$

where H_x , H_y , B_x , and B_y are the field strength and flux density, respectively, at the point considered on the transformer steel sheet.

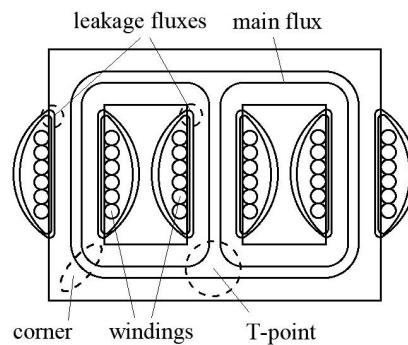


Fig. 1. Example of magnetic field lines in three-phase transformer core

Owing to their Goss texture (Fig. 2), transformer sheets are typically anisotropic sheets [1–6]. This renders the determination of the magnetic field in these sheets when the direction of the field strength differs from the rolling direction (RD) or the transverse direction (TD) challenging.

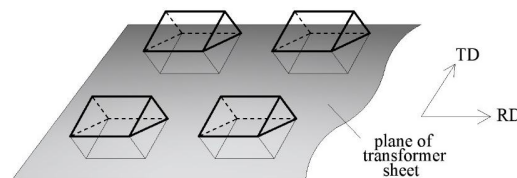


Fig. 2. Section of transformer sheet with Goss texture

Because of their anisotropic properties, the hysteresis loops differ significantly for individual magnetisation directions. For magnetisation angles exceeding approximately 54° , their shape is significantly different compared to the ‘classical’ hysteresis shape (Fig. 3). Consequently, the determination of the magnetic field in the corners and T-joint areas is difficult, because the directions of the magnetic field strength differ at individual points of the transformer core. This would necessitate the storage of a significant number of measured hysteresis loops in computer memory.

The problem of determining losses in transformer cores is still up to date [7–11]. Professional software considers the nonlinearity and anisotropy of electrical sheets [12]; however, these software packages cannot be applied to magnetic hysteresis because they are based on Maxwell’s equations in differential form. If these equations are based on Maxwell’s equations in integral form, the magnetic

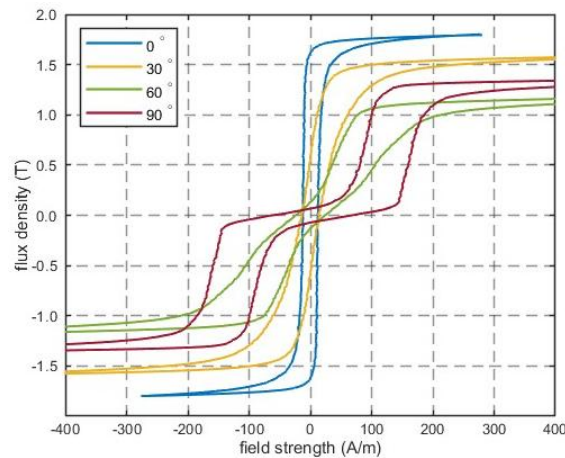


Fig. 3. Examples of hysteresis loops of M120-27S-type transformer sheet

hysteresis can be directly included in the equations of the magnetic field distribution if these equations are based on Maxwell's equations in the integral form [13]. This study proposed a new method for considering the hysteresis phenomenon by determining the resultant flux density at individual points as the geometric sum of the flux densities along both the rolling and transverse directions.

2. Magnetisation process in transformer sheets

The magnetisation process is dependent on the direction and value of the field strength [14]. If the magnetisation direction approaches the RD, then the direction of the resultant flux density vector approaches the RD (Fig. 4(a)). However, when the magnetisation approaches the TD, the resultant flux density vector increases along the RD only in the initial phase (Fig. 4(b)). Digits 1–8 in Fig. 4 indicate the subsequent positions the end of the resultant flux density vector. For low field strength values, the direction of the resultant flux density vector approaches the RD (point 1). If the magnetisation direction is relatively close to the TD, the resultant flux density vector may be located on both sides of the magnetisation direction. This magnetisation process is owing to the 'disintegration' of domains whose flux density vectors approach the RD and the growth of domains whose flux density vectors are parallel to the TD [14].

The magnetisation process in iron crystals (Fig. 5) involving the reconstruction of the domain structure first occurs along the easy magnetisation axes [15–19]. The intensity of this reconstruction significantly depends on the direction of magnetisation. If the angle between this direction and the RD is less than 54.7° , changes in the flux density occur mainly along the RD; otherwise, changes occur along the other two axes of easy magnetisation.

The resultant flux density vector is the geometric sum of the flux densities along the RD and TD (Fig. 6). However, the changes in the flux densities along these directions cannot be determined based on the loops measured in these directions. Therefore, the hysteresis loops should be defined along the RD and TD for different magnetisation directions.

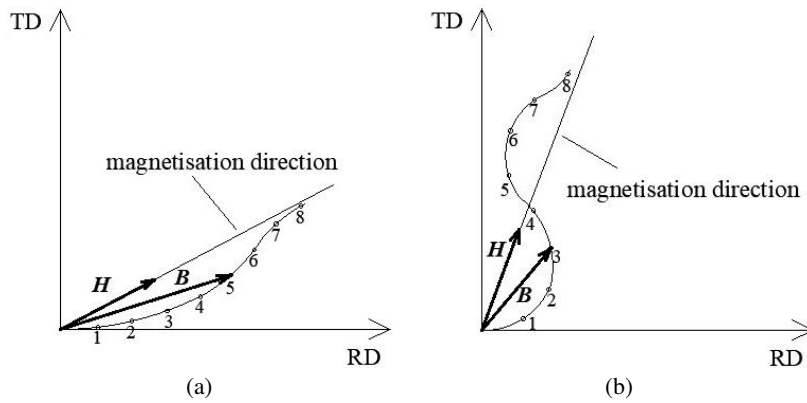


Fig. 4. Changes in resultant flux density when magnetisation approaches: RD (a); TD (b); digits indicate successive positions of resultant flux density vector for increasing field strength

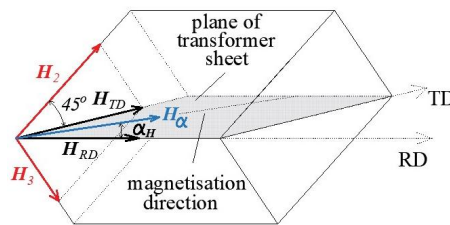


Fig. 5. Field strength components H_{RD} , H_2 , and H_3 along the easy magnetisation axes: H_α – field strength along magnetisation direction, H_{TD} – field strength component along TD

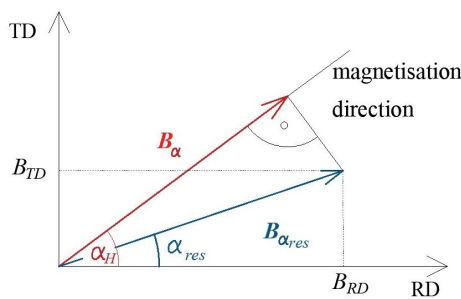


Fig. 6. Components of flux density on sheet plane

3. Model of magnetisation process in transformer sheets

The magnetisation direction significantly influences the changes in the flux density. As previously mentioned, when the angle between this direction and the RD is less than 54.7° , these changes occur primarily along the axis parallel to the RD; otherwise, they occur along the two other axes of easy magnetisation. Therefore, the limiting hysteresis loops $B = f(H)$ related to the easy magnetisation axes should be modified according to the direction of magnetisation [20].

However, these limiting hysteresis loops cannot be measured, and their shapes depend on the direction of magnetisation. Figure 7 shows examples of the limiting hysteresis loops along the RD and TD for three magnetisation angles α_H .

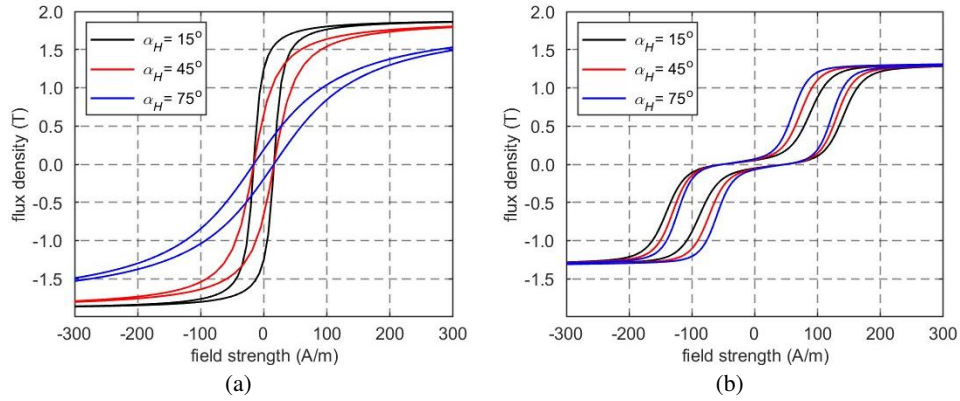


Fig. 7. Limiting hysteresis loops for three magnetisation angles α_H along: RD (a); TD (b)

Knowledge of the limiting loops is necessary to determine the flux density related to the minor loops for any field strength. The changes in the flux density (Fig. 8) can be expressed as follows [13]:

$$B = B_b + \Delta B_r \exp[-k_{B_r}(H - H_0)], \quad (2)$$

if H increases, or

$$B = B_u - \Delta B_d \exp[k_{B_d}(H - H_0)], \quad (3)$$

if H decreases,

where B_b and B_u denote bottom and upper curves of the limiting hysteresis loop, respectively, and k_{B_r} and k_{B_d} denote the attenuation coefficients for increasing and decreasing H , respectively.

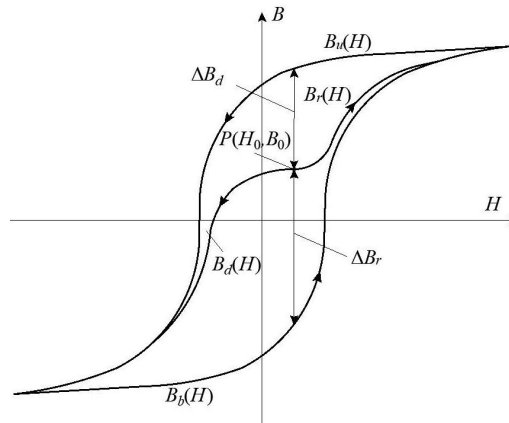


Fig. 8. Possible trajectories of point $P(H_0, B_0)$ inside the limiting hysteresis loop

For a certain field strength H_α (Fig. 5), the field strength components H_{RD} and H_{TD} were determined, and based on the loops $B_{RD} = f(H_{RD})$ and $B_{TD} = f(H_{TD})$ the resultant flux densities were estimated. However, in the magnetic field distribution equations, only the flux densities B_{RD} and B_{TD} should be introduced, as described in the next Section. Notably, in the corners, T-joint areas, and particularly in the areas where the leakage flux is closed by air (Fig. 1), the direction of the magnetic field strength changes according to the winding currents; these changes are significant when the saturation state is achieved. In a different field strength direction, new curves $B_b(H)$ and $B_u(H)$ of the limiting hysteresis loop should be determined, and changes in the flux density B_r or B_d should be calculated using (2) and (3).

4. Equations of magnetic field distribution

The field occurrence must be divided into elementary segments. The field strength components H_p are assigned to the branches belonging to the graph tree, which include the dependent branches. The components H_m are associated with branches that do not belong to the graph tree (Fig. 9) and the superscripts denote the branch number. For each field strength component along the x -axis, two flux density components are assigned; whereas, the component with index a lies above the branch with the corresponding field strength component, and those with index b are located below the branch with this field strength component. However, owing to the nonlinearity and anisotropy of the transformer sheets, the flux density components are located in segments with different magnetic properties. Similarly, the flux density components with index l are located on the left side of the corresponding field strength component, and those with index r are placed on the right side of the field strength component. A detailed description of the individual components has been extensively reported in [21]. A graph tree containing dependent and independent branches must be determined to assign components to individual branches that divide the area of the magnetic field. Notably, the directions of all components were parallel to the rolling or transverse directions.

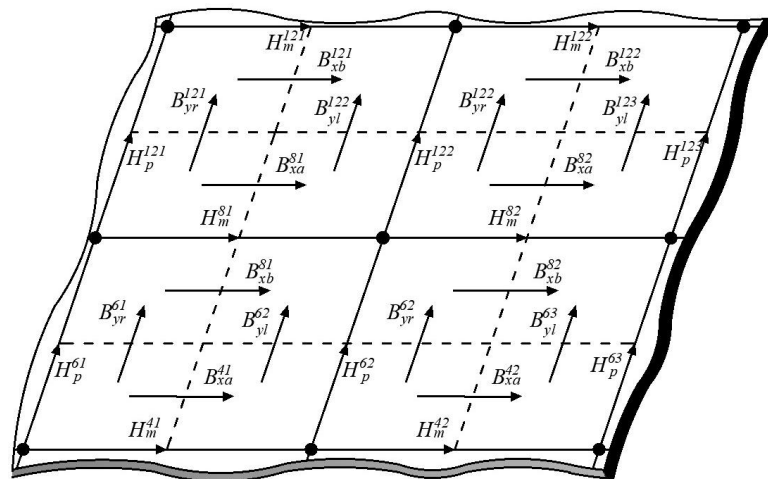


Fig. 9. Example of assignment of components to mesh edges and elementary segments

The matrix equations for the independent meshes were formulated based on the first Maxwell equation [21]:

$$\mathbf{A}_m \mathbf{H}_m + \mathbf{A}_p \mathbf{H}_p = \mathbf{S}_J \mathbf{J}_{\text{ex}}, \quad (4)$$

where: \mathbf{H}_m and \mathbf{H}_p are the column vectors of the magnetic field strength components that are assigned to the independent or dependent branches of the graph tree, respectively, \mathbf{A}_m and \mathbf{A}_p are the matrices of geometric dimensions, \mathbf{S}_J denotes the matrix of the surfaces of elementary segments, and \mathbf{J}_{ex} denotes the column vector of the density values of external currents.

The components of the vector \mathbf{H}_m are the field strength H_{RD} , whereas vector \mathbf{H}_p contains the components H_{TD} and partially components H_{RD} related to the branches belonging to the graph tree.

Using the Gauss law, the algebraic matrix equation was formulated as [21]:

$$\mathbf{C}_{xa} \mathbf{B}_{xa} + \mathbf{C}_{xb} \mathbf{B}_{xb} + \mathbf{C}_{yl} \mathbf{B}_{yl} + \mathbf{C}_{yr} \mathbf{B}_{yr} = 0, \quad (5)$$

where \mathbf{B}_{xa} , \mathbf{B}_{xb} , \mathbf{B}_{yl} , and \mathbf{B}_{yr} are the column vectors of the flux density components and \mathbf{C}_{xa} , \mathbf{C}_{xb} , \mathbf{C}_{yl} , and \mathbf{C}_{yr} are the matrices of the segment face areas.

The flux density components were placed in column vectors depending on whether they referred to the independent or dependent branches of the graph tree. The vectors \mathbf{B}_{xa} and \mathbf{B}_{xb} included only the flux densities that were assigned to the independent branches of the graph tree; further, these flux density components were parallel to the RD. However, the vectors \mathbf{B}_{yl} and \mathbf{B}_{yr} contained all the flux densities parallel to the TD and partially components along the RD, and all components of these column vectors were assigned to dependent branches. In general, the components of the column vectors of the flux density are functions of the field strength components \mathbf{H}_m or \mathbf{H}_p :

$$\mathbf{B}_{xa} = f(\mathbf{M}_{xam} \mathbf{H}_m, \mathbf{M}_{xap} \mathbf{H}_p), \mathbf{B}_{xb} = f(\mathbf{M}_{xbm} \mathbf{H}_m, \mathbf{M}_{xbp} \mathbf{H}_p), \quad (6a)$$

$$\mathbf{B}_{yl} = f(\mathbf{M}_{ylm} \mathbf{H}_m, \mathbf{M}_{ylp} \mathbf{H}_p), \mathbf{B}_{yr} = f(\mathbf{M}_{yrm} \mathbf{H}_m, \mathbf{M}_{yrp} \mathbf{H}_p), \quad (6b)$$

where: \mathbf{M} -type matrices determine the appropriate field strength component to which a particular flux density component is assigned, and f denotes nonlinear functions describing changes in the flux density components depending on the corresponding field strength components. The method of considering the hysteresis phenomenon was widely described in [20].

Based on (4), the column vector \mathbf{H}_m can be replaced with \mathbf{H}_p :

$$\mathbf{H}_m = \mathbf{A}_m^{-1} (\mathbf{S}_J \mathbf{J}_{\text{ex}} - \mathbf{A}_p \mathbf{H}_p). \quad (7)$$

Finally, a nonlinear matrix equation was formulated wherein the vector \mathbf{H}_p is unknown:

$$\begin{aligned} & \mathbf{C}_{xa} f(\mathbf{M}_{xam} \mathbf{A}_m^{-1} (\mathbf{S}_J \mathbf{J}_{\text{ex}} - \mathbf{A}_p \mathbf{H}_p), \mathbf{M}_{xap} \mathbf{H}_p) + \mathbf{C}_{xb} f(\mathbf{M}_{xbm} \mathbf{A}_m^{-1} (\mathbf{S}_J \mathbf{J}_{\text{ex}} - \mathbf{A}_p \mathbf{H}_p), \mathbf{M}_{xbp} \mathbf{H}_p) \\ & + \mathbf{C}_{yl} f(\mathbf{M}_{ylm} \mathbf{A}_m^{-1} (\mathbf{S}_J \mathbf{J}_{\text{ex}} - \mathbf{A}_p \mathbf{H}_p), \mathbf{M}_{ylp} \mathbf{H}_p) + \mathbf{C}_{yr} f(\mathbf{M}_{yrm} \mathbf{A}_m^{-1} (\mathbf{S}_J \mathbf{J}_{\text{ex}} - \mathbf{A}_p \mathbf{H}_p), \mathbf{M}_{yrp} \mathbf{H}_p) = 0. \end{aligned} \quad (8)$$

The Newton–Raphson method was used to solve (8) for a particular value of external current. Thereafter, the values of the field strength and flux density components in individual elementary segments were calculated, and the directions of the field strength changes in individual elementary segments were determined. For new directions of the field strength, the coefficients for the limiting hysteresis loops were introduced into the relationships between the flux density components and the field strength, and (8) was solved for the subsequent values of the external current. Changing

the direction of the field strength implies that other limiting hysteresis loops should be included to calculate the changes in the flux density in the individual segments [13]. The condition of flux density saturation in individual elementary segments was considered in the numerical calculations.

The most appropriate validation of the correctness of (8) is a comparison of the changes in the flux density with respect to that in the field strength. However, measuring the field strength of transformer sheets is challenging. For this purpose, two flat measuring coils that are as thin as possible should be applied to the sheet in the rolling and transverse directions [1]. The principle involved is that the tangential component of the field strength does not change its value at the sheet-air boundary. Numerical calculations, conducted using FEMM, showed that the tangential component of the flux density was approximately 0.3 mT at a distance of 0.5 mm from the sheet surface when the flux density in the tested transformer sheet was 1.0 T. The voltage induced in the measuring coils used to determine the field strength was approximately 1.5 mV, which did not facilitate such measurement signals to be considered reliable. Therefore, the accuracy of the equations was indirectly verified.

The proposed equation was validated using a transformer sheet package (Fig. 10). The magnetic field was excited by two mutually perpendicular coils supplied with a sinusoidal current at a frequency of 10 Hz to avoid the influence of eddy currents occurring in the transformer sheets. The measuring coils contained three turns and were placed at the centre of the sheet package. Consequently, changes in flux density were determined using Faraday's law based on the voltages recorded by the measuring coils.

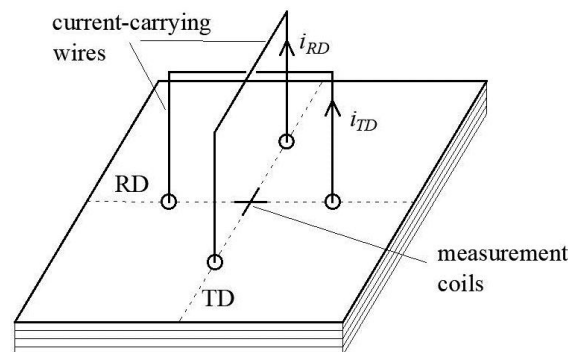


Fig. 10. Measurement system for indirect validation of correctness of magnetic field equation

The static hysteresis loop became dynamic because of the occurrence of eddy currents. The difference between these loops primarily was dependent on the winding current frequency. Figure 11 shows the hysteresis loops for the four frequencies. The frequency of changes in the magnetic field should be as low as possible to eliminate the influence of eddy currents; however, it should be sufficiently high to render the voltage signals recorded by the measuring coils useful.

Measurements and calculations were also performed for the same current values as previously used for frequencies of 5, 20, 30, 40, and 50 Hz to assess the influence of eddy currents. For individual frequencies, the amplitudes of the flux density changes along the direction of RD were determined for currents of 3 and 6 A (Table 1). The amplitude of the flux density for a frequency of 10 Hz and a current of 3 A was 0.01 T (approximately 1.2%) lower than the amplitude at 5 Hz.

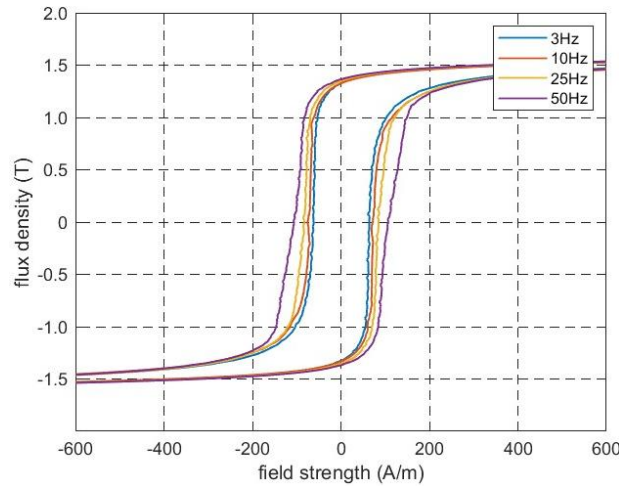


Fig. 11. Hysteresis loops measured for four frequencies

For frequencies higher than 10 Hz, the changes in the amplitude were significant owing to the influence of eddy currents. The differences in the amplitudes of the flux density were smaller for a current of 6 A; however, the flux density in the centre of the sheet package reached the maximum value. This was attributed to the saturation in the transformer sheets around the wires carrying the current. Owing to small differences in the flux density amplitudes for frequencies of 5 and 10 Hz, verification measurements were performed for 10 Hz because the signals from the measuring coils were very disturbed at 5 Hz.

Table 1. Amplitudes B_{\max} of flux density along RD for two current

Frequency	5	10	20	30	40	50	60	Hz
$B_{\max}(3\text{ A})$	0.86	0.85	0.78	0.71	0.66	0.61	0.58	T
$B_{\max}(6\text{ A})$	1.42	1.41	1.40	1.39	1.38	1.37	1.36	T

The tests were performed for two currents supplying the windings and generating a magnetic field along the RD and TD. During the tests, the voltages in the measuring coils were recorded and compared with the corresponding voltages calculated numerically under the same conditions as those in the experiment (Figs. 12, 13, and 14). Figure 12 shows the calculated and measured voltages when the magnetic field was excited along the RD for currents of 3 and 6 A (RMS values). The measured flux densities were determined by integrating the voltages of the measuring coils. Figure 13 shows the analogous voltages when the magnetic field occurred along the TD for the same currents.

In the latter case, both the windings were connected in series. The voltages of the measurement coils were also recorded for currents of 3 and 6 A, and the subsequent changes in the flux density in both characteristic directions were determined (Fig. 14). At a current of 3 A, the changes in the flux density were approximately the same for both the magnetisation directions. However, at

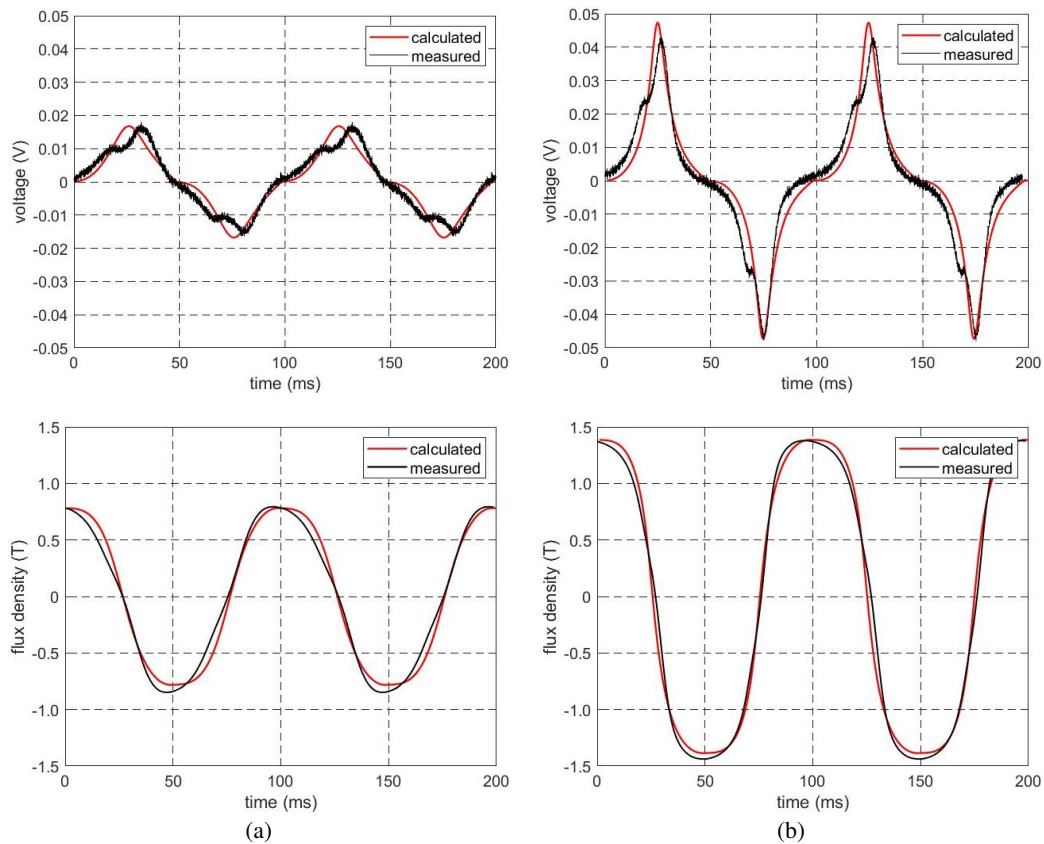


Fig. 12. Measured (black) and calculated (red) voltages and flux densities when magnetic field was excited along RD for coil currents of: 3 A (a); 6 A (b)

a current of 6 A, the flux densities in both the RD and TD were significantly lower than those in each direction when the windings were supplied separately. This was attributed to the condition that the sum of the flux densities along the RD and TD could not exceed the saturation flux density of the tested transformer sheet.

Methods for determining the magnetic field distribution based on Maxwell's equations in differential form do not allow the hysteresis phenomenon to be considered directly. In certain cases, magnetic hysteresis is considered in the calculations when a stable solution is obtained in a given simulation step. The curves $B = f(H)$ are then modified accordingly for the next step of the calculations; however, this may result in significant errors. In the proposed method, the relationships describing the changes in flux density with respect to field strength changes were directly introduced into the equation describing the magnetic field distribution.

The described method can be used to analyse the magnetic field in dynamo steel sheets, particularly because these sheets exhibit isotropic properties or are characterised by slight anisotropy. Therefore, considering the phenomenon of magnetic hysteresis is much simpler than in transformer sheets.

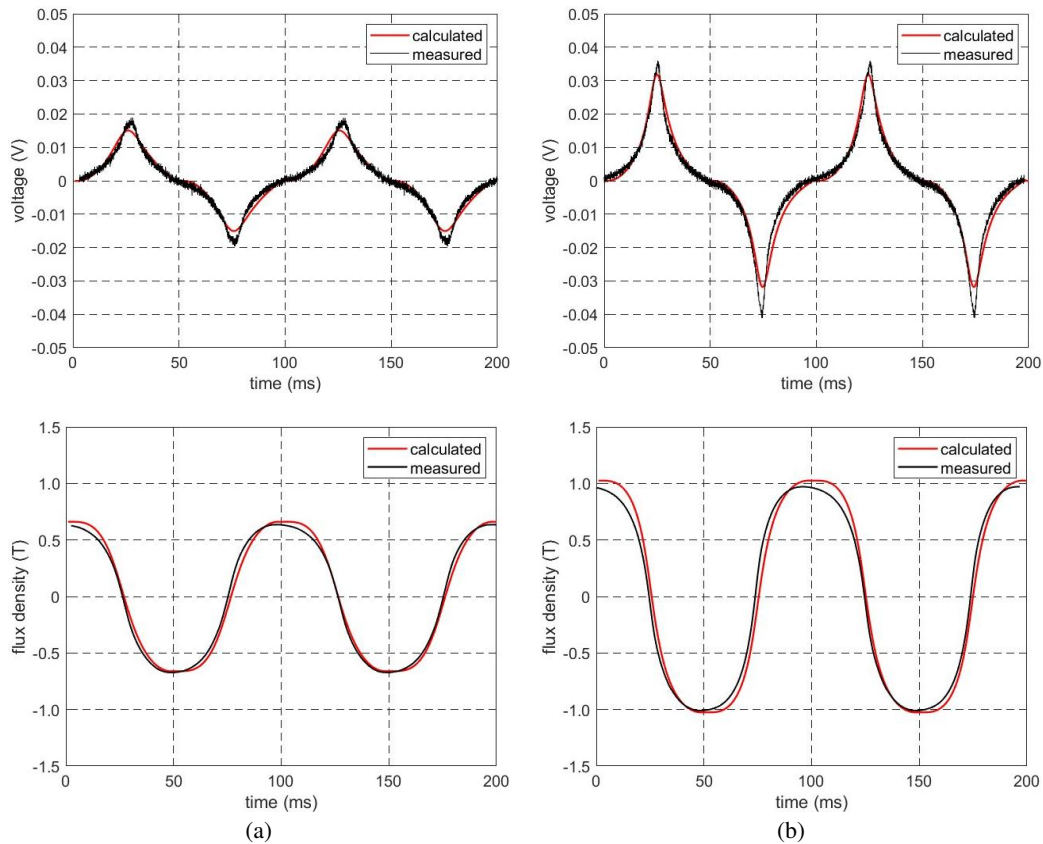


Fig. 13. Measured (black) and calculated (red) voltages and flux densities when magnetic field was excited along TD for coil currents of: 3 A (a); 6 A (b)

The calculation times using the proposed method were much longer than those using nonlinear but unambiguous magnetisation characteristics, that is, without considering magnetic hysteresis. Therefore, the authors suggest using the proposed method to calculate the magnetic field in the corners, particularly in areas of the T-joint points of transformer cores, because magnetic hysteresis causes elliptical rotational magnetisation and higher power losses in these areas. The proposed method can be used to calculate the magnetic field in the entire transformer core, particularly if the number of elementary segments dividing the area of the columns and yokes can be reduced, that is if the magnetic field can be regarded as a one-dimensional field.

Notably, the described method does not facilitate the use of elementary segments other than rectangular segments. This is inconvenient when dividing the magnetic field area, which requires local mesh refinement. Another significant problem is matrix scaling, particularly with numerous elementary segments, which often results in an unstable solution of the nonlinear system of algebraic equations.

The described method cannot be directly used to analyse transients owing to eddy currents. The measurements showed that at a frequency of 10 Hz the phase shift between the first harmonic of the flux density and the current of 3 A was about 23° , and about 15° at a current of 6 A. The

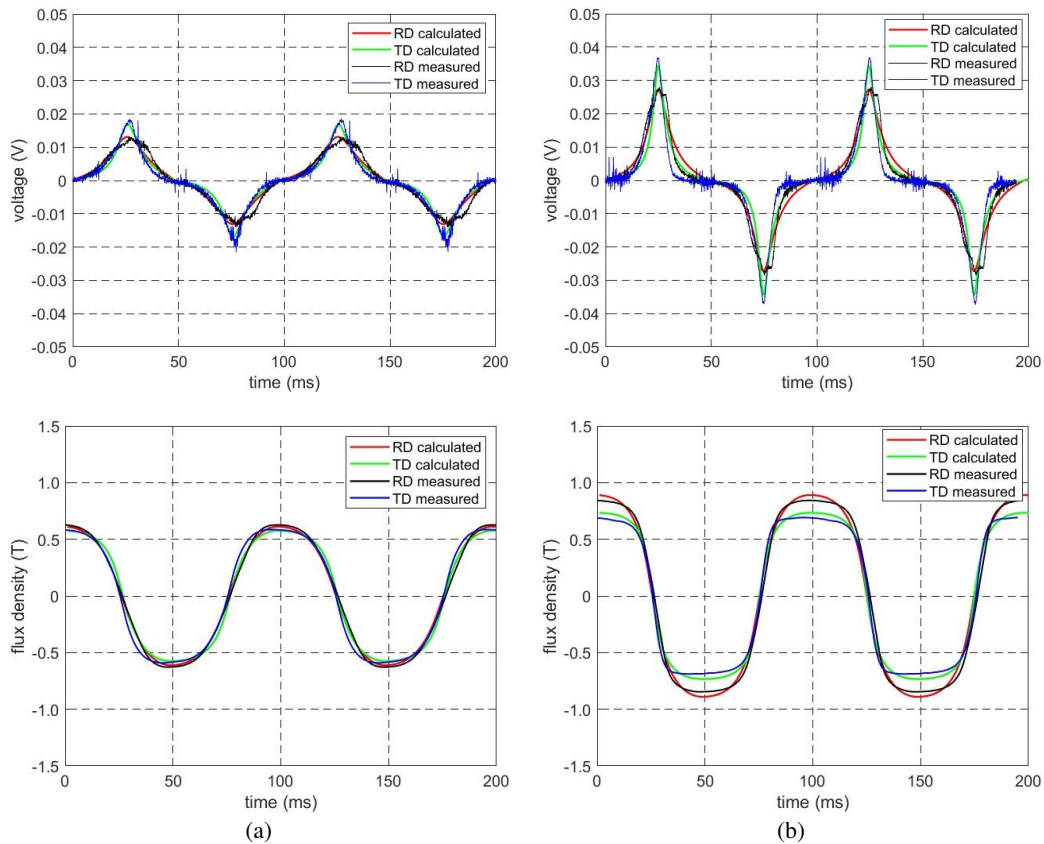


Fig. 14. Measured and calculated voltages and flux densities when both windings were connected in series for currents of: 3 A (a); 6 A (b); red and green lines indicate calculated changes along RD and TD, respectively, black and blue lines indicate measured changes along RD and TD, respectively

eddy currents can be considered by creating a separate resistive or conductive grid. Both grids must be mutually coupled because changes in the magnetic field influence changes in the eddy currents and vice versa [22–24].

5. Conclusions

This study employed a method based on Maxwell’s equations in the integral form to determine the magnetic field distribution in the transformer sheets. This approach rendered the consideration of the hysteresis changes along the rolling and transverse directions relatively easier because both the field strength and flux density components were defined along these directions. The proposed approach facilitated the determination of changes in the flux density in any direction and the value of the magnetic field strength at any point on the tested transformer sheet.

The field strength components estimated in a given calculation step enabled the determination of the directions of the field strength in individual elementary segments for the next value of the current exciting the magnetic field. This is important for calculating the field distribution in the corners and T-joint areas, and consequently for determining the areas wherein the losses are much higher than in columns or yokes.

The magnetic field equation was indirectly validated because changes in the field strength in the laboratory package were not recorded. Despite the consistency between the measured and calculated voltage waveforms of the measuring coils, future studies must simultaneously measure the magnetic field strength for different values of the currents exciting the magnetic field.

References

- [1] Tumański S., *Handbook of Magnetic Measurements*, CRC Press: Boca Raton (2011).
- [2] Bozorth R.M., *Ferromagnetism*, IEEE Press, New York (1978).
- [3] Iványi A., *Hysteresis models in electromagnetic computation*, Akadémiai Kiadó, Budapest (1997).
- [4] Jiles D., *Introduction to Magnetism and Magnetic Materials*, Chapman & Hall, London (1998).
- [5] Tumański S., *Investigations of the anisotropic behaviour of SiFe Steel*, Journal of Magnetism and Magnetic Materials, vol. 254–255, pp. 50–53 (2003), DOI: [10.1016/S0304-8853\(02\)00745-X](https://doi.org/10.1016/S0304-8853(02)00745-X).
- [6] Beckley P., *Electrical steels for rotating machines*, Bell & Bain Ltd., Glasgow (2002).
- [7] Mousavi S., Shamei M., Siadatan A., Nabizadeh F., Mirimani S.H., *Calculation of Power Transformer Losses by Finite Element Method*, IEEE Electrical Power and Energy Conference, EPEC (2018), DOI: [10.1109/EPEC.2018.8598292](https://doi.org/10.1109/EPEC.2018.8598292).
- [8] Sarac V., *FEM 2D and 3D design of transformer for core losses computation*, International Scientific Journal – Machines. Technologies. Materials, vol. 2, no. 3, pp. 119–122 (2017).
- [9] Baron B., Kolańska-Pluska J., Łukaniszyn M., Spalek D., Kraszewski T., *Solution of nonlinear stiff differential equations for a three-phase no-load transformer using a Runge–Kutta implicit method*, Archives of Electrical Engineering, vol. 71, no. (4), pp. 1081–1106 (2022), DOI: [10.24425/aee.2022.142126](https://doi.org/10.24425/aee.2022.142126).
- [10] Chen R., Martin F., Li Y., Yue S., Belahcen A., *An Energy-based Anisotropic Vector Hysteresis Model for Rotational Electromagnetic Core Loss*, IEEE Transactions on Industrial Electronics, vol. 71, no. 6, pp. 6084–6094 (2024), DOI: [10.1109/TIE.2023.3294635](https://doi.org/10.1109/TIE.2023.3294635).
- [11] Jabłoński P., Najgebauer M., Bereźnicki M., *An Improved Approach to Calculate Eddy Current Loss in Soft Magnetic Materials Based on Measured Hysteresis Loops*, Energies, vol. 15, no. 8 (2022), DOI: [10.3390/en15082869](https://doi.org/10.3390/en15082869).
- [12] Mikula L., Ramdane B., Blatter Martinho L., Kedous-Lebouc A., Meunier G., *Numerical modelling of static hysteresis phenomena using a vector extension of the Loss Surface model*, IEEE Conference on Electromagnetic Field Computation, CEFC (2022), DOI: [10.1109/CEFC55061.2022.9940905](https://doi.org/10.1109/CEFC55061.2022.9940905).
- [13] Mazgaj W., Sierzega M., Szular Z., *Approximation of Hysteresis Changes in Electrical Steel Sheets*, Energies, vol. 14, no. 14 (2021), DOI: [10.3390/en14144110](https://doi.org/10.3390/en14144110).
- [14] Pfützner H., *Rotational Magnetisation and Rotational Losses of Grain Oriented Silicon Steel Sheets – Fundamental Aspects and Theory*, IEEE Transactions on Magnetics, vol. 30, no. 5, pp. 2802–2807 (1994), DOI: [10.1109/20.312522](https://doi.org/10.1109/20.312522).
- [15] Mao W., Atherton D.L., *Magnetisation Vector Directions in a Steel Cube*, IEEE Transactions on Magnetics, vol. 36, no. 5, pp. 3084–3086 (2000), DOI: [10.1109/20.908688](https://doi.org/10.1109/20.908688).
- [16] Shin S., Schaefer R., DeCooman B.C., *Anisotropic magnetic properties and domain structure in Fe-3%Si(110) steel sheet*, Journal of Applied Physics, vol. 109, no. 7, 07A307 (2011), DOI: [10.1063/1.3535547](https://doi.org/10.1063/1.3535547).

- [17] Sudo M., Matsuo T., *Magnetisation modeling of silicon steel using a simplified domain structure model*, Journal of Applied Physics, vol. 111, no. 7, 07D107 (2012), DOI: [10.1063/1.3672073](https://doi.org/10.1063/1.3672073).
- [18] Furuya A., Fujisaki J., Uehara Y., Shimizu K., Oshima H., Matsuo., *Micromagnetic Hysteresis Model Dealing with Magnetisation Flip Motion for Grain-Oriented Silicon Steel*, IEEE Transactions on Magnetics, vol. 50, no. 11 (2014), DOI: [10.1109/TMAG.2014.2329679](https://doi.org/10.1109/TMAG.2014.2329679).
- [19] Fiorillo L., Dupré R., Appino C., Rietto A.M., *Comprehensive model of magnetisation curve, hysteresis loops, and losses in any direction in grain-oriented Fe-Si*, IEEE Transactions on Magnetics, vol. 38, no. 3, pp. 1467–1475 (2002), DOI: [10.1109/20.999119](https://doi.org/10.1109/20.999119).
- [20] Sierżęga M., Mazgaj W., *Modelling of magnetisation processes in transformer steel sheets*, Archives of Electrical Engineering, vol. 72, no. 4, pp. 855–870 (2023), DOI: [10.24425/ae.2023.147415](https://doi.org/10.24425/ae.2023.147415).
- [21] Warzecha A., Mazgaj W., *Magnetisation measurements in circle-shaped samples of typical dynamo steel sheets*, Przegląd Elektrotechniczny, no. 6 (2015), DOI: [10.15199/48.2015.06.19](https://doi.org/10.15199/48.2015.06.19).
- [22] Albanese R., Rubinacci G., Canali M., Stangherlin S., Musolino A., Raugi M., *Analysis of a Transient Nonlinear 3-D Eddy Current Problem with Differential and Integral Methods*, IEEE Transactions on Magnetics, vol. 32, no. 3, pp. 776–779 (1996), DOI: [10.1109/20.497355](https://doi.org/10.1109/20.497355).
- [23] Demenko A., *Three Dimensional Eddy Current Calculation Using Reluctance-Conductance Network Formed by Means of FE Method*, IEEE Transactions on Magnetics, vol. 36, no. 4, pp. 741–745 (2000), DOI: [10.1109/20.877554](https://doi.org/10.1109/20.877554).
- [24] Szular Z., Mazgaj W., *Calculations of eddy currents in electrical steel sheets taking into account their magnetic hysteresis*, COMPEL, no. 38, pp. 1263–1273 (2019), DOI: [10.1108/COMPEL-10-2018-0424](https://doi.org/10.1108/COMPEL-10-2018-0424).